Penerbit Akademia Baru

Journal of Advanced Research Design
ISSN (online): 2289-7984 | Vol. 4, No.1. Pages 20-27, 2015

Numerical Study of Turbulent Flow over Backward-Facing Step with Different Turbulence Models

D. G. Jehad [*,a], *G. A. Hashim*[b], *A. K. Zarzoor*[c] *and C. S. Nor Azwadi*[d]

Department of Thermo-Fluids, Faculty of Mechanical Engineering, Universiti Teknologi Malaysia, 83100 Skudai, Johor Bahru, Malaysia

[a,*]*dhafir_alalwan@yahoo.com,* [b]*ghasaq_88@yahoo.com,* [c]*ahmedmechano1@gmail.com,* [d]*azwadi@fkm.utm.my*

Abstract – *Numerical studies are conducted on turbulent incompressible flow over 2D backward-facing step in order to investigate the performance of three different turbulence models (standard k-e, realizable k-e and SST k-ω) in predicting the region of separation and reattachment behind the edge of the step. Current solutions of Reynolds number (Re= 13200) and expansion ratio (H: H2=1:3) are compared with experimental measurements. Among the turbulence models, SST k-ω and standard k-e exhibited good agreement with the experimental results.*

Keywords: Turbulence model, Turbulent flow, Backward-facing step, Separation, Reattachment

1.0 INTRODUCTION

Flow over a backward-facing step is accounted as a major reason for the generation of recirculation zones and formation of vortices because of flow separation occurring from counter pressure gradients in the flow of fluid [4]. The fluid flow over a backward-facing step has become a subject of interest in which the separation and reattachment processes of turbulent shear layers can be investigated in various practical engineering applications such as internal flow systems (e.g. combustors, diffusers) and flow over airfoils and buildings [1-2]. The two-dimensional (2-D) backward-facing step gives a superior state for investigating the fundamental physical phenomena of separation and reattachment due to its geometrical simplicity [3]. This flow is also considered as an important test that can be employed in order to compare between the turbulence models. With redundancy of data in literature, the flow over a backward facing step is frequently employed as a benchmark test case for several CFD codes and models related to turbulent flows. A variety of turbulence models such as RANS, LES and DNS have all been employed to simulate this flow in 2D domains and in 3D as well [5].

Armaly et al. [3] studied a backward-facing step flow both experimentally and numerically. From their results, they noticed a variance in the lengths of major recirculation obtained from the experimental and the numerical works. In addition, they observed a region of secondary flow at the upper wall of the channel. Eaton and Johnston [6] investigated experimentally the separation of flow back, a rearward facing step. A vortex module was noticed in the layer of free shear as the separating boundary layer was turbulent. Lee and Mateescu [8] conducted an

Journal of Advanced Research Design
ISSN (online): 2289-7984 | Vol. 4, No.1. Pages 20-27, 2015

experimental and numerical study of air flow over a two-dimensional backward-facing step. They noticed good agreement between the numerical and experimental results in terms of the position of the separation and reattachment points. Le et al. [9] studied turbulent flows past a backward-facing step, numerically. The immediate velocity domain showed the change of reattachment lengths in the spanwise direction and the flow also showed the robust structure of a streamwise vortex. Sinha et al. [7] investigated the turbulent region past a backward-facing step. They noticed that for Re higher than 10,000, the region of re-attachment almost becomes a fixed value step height. Adams and Johnston [10] investigated the flow over a backward facing step, experimentally. They found that the length of reattachment for the case of turbulent boundary layers, upstream of the step, was higher compared to the laminar upstream boundary layers. Scarano and Reithmuller [32] investigated the recirculation region characteristics behind a backward-facing step. They found that the main vortex stretched from the edge of the step to the point of reattachment whereas the counter-rotating secondary vortex remains in the corner of the step wall. However in the present work, the main goal is to analyze and compare the separation and reattachment regions of the flow over a 2D backward-facing step based on three different turbulent models (standard k-$\mathcal{E}$, realizable k-$\mathcal{E}$ and SST k-ω)

2.0 MATHEMATICAL MODELLING

2.1 Problem definition

A schematic view of a 2D backward facing step is shown in Fig. 1 [13]. The flow entering from the left side dissociates at the sharp corner of the step thereafter, reattaches again to the lower wall at a distance L, behind the step. A recirculation region is subsequently produced directly behind the step. The expansion ratio that represents the step height (H) to outlet channel height (H2) is 1:3 while the Reynolds number is 13,200.

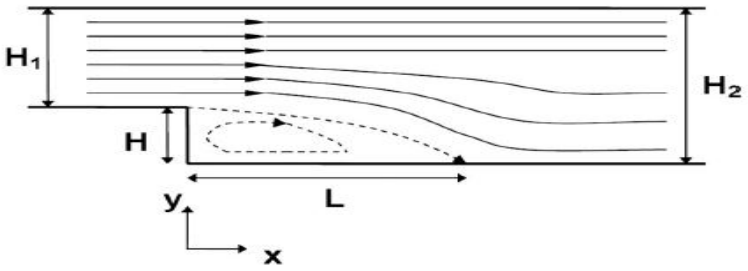

Figure 1: Geometry and flow style of the backward-facing step

2.2 Governing equations

The equations of conservation of mass and momentum in the case of incompressible and stationary turbulence can be written in Cartesian-tensor notation as

$$\frac{\partial U_i}{\partial x_i} = 0 \qquad (1)$$

Journal of Advanced Research Design
ISSN (online): 2289-7984 | Vol. 4, No.1. Pages 20-27, 2015

$$U_j \frac{\partial U_i}{\partial x_j} = -\frac{1}{\rho}\frac{\partial p}{\partial x_i} + \frac{\partial}{\partial x_j}\left(v\left(\frac{\partial U_i}{\partial x_j} + \frac{\partial U_j}{\partial x_j}\right) - \overline{u_i' u_j'}\right) \quad (2)$$

The term $\overline{u_i' u_j'}$ is known as the Reynolds-stress tensor and has to be determined with a turbulence model.

2.3 Turbulence modelling

Different turbulence models can be employed to compute a solution of the governing equations. In this work, in order to analyze the turbulent flow over the 2D backward facing step in terms of separation and reattachment, three turbulent models (standard k-e, realizable k-e and SST k-w) are implemented.

2.3.1 The standard k-ε model

The correlations of this model are [11]:

$$U_i \frac{\partial k}{\partial x_i} - \frac{\partial}{\partial x_i}\left[\frac{v_T}{\sigma_k}\frac{\partial k}{\partial x_i}\right] = P - \varepsilon, \quad (3)$$

$$U_j \frac{\partial \varepsilon}{\partial x_j} - \frac{\partial}{\partial x_i}\left[\frac{v_T}{\sigma_\varepsilon}\frac{\partial \varepsilon}{\partial x_i}\right] = \frac{\varepsilon}{k}(C_{\varepsilon 1}P - C_{\varepsilon 2}\varepsilon), \quad (4)$$

$$v_T = C_\mu \frac{k^2}{\varepsilon}, \quad (5)$$

$$P_k = -\overline{u_i' u_j'}\left(\frac{\partial U_j}{\partial x_i} + \frac{\partial U_i}{\partial x_j}\right), \quad (6)$$

$$\overline{u_i' u_j'} = \frac{2}{3}\delta_{ij}k - v_T\left(\frac{\partial U_j}{\partial x_i} + \frac{\partial U_i}{\partial x_j}\right) \quad (7)$$

where; C_μ=0.09, $C_{\varepsilon 1}$=1.44, $C_{\varepsilon 2}$=1.92, σ_k = 1and σ_ε = 1.3 are the constants of the model while P_k signifies the production rate of the turbulence kinetic energy. v_T is the Boussinesq eddy viscosity, while the turbulence Reynolds stress tensor is calculated with the help of the generalized Boussinesq hypothesis (Eq. (5)).

2.3.2 The realizable *k–ε* model (RKE)

The k equation is identical with the standard k–ε and ε equations, and is given by

$$\frac{\partial U_j \varepsilon}{\partial x_j} = \left(\mu + \frac{\mu_t}{\sigma_\varepsilon}\right)\nabla^2\varepsilon + C_1 S\rho\varepsilon - C_2\frac{\rho\varepsilon^2}{k+\sqrt{v\varepsilon}}, \quad (8)$$

where; C_1=max[0.43,η/(η+5)], C_2= 1.0, σ_k= 1.0, σ_ε=1.2

$\eta = Sk/\varepsilon$, η: represents the ratio between the time scales of the turbulence and the mean flow.

$S = \sqrt{2S_{ij}S_{ij}}$, S denotes the mean strain-rate of the flow, Sij; the deformation tensor.

2.3.3 The SST (shear stress transport) k-ω Turbulence Model

The formulation of SST k-ω is given by [12] as follows

Journal of Advanced Research Design
ISSN (online): 2289-7984 | Vol. 4, No.1. Pages 20-27, 2015

Turbulent kinetic energy:

$$U_i \frac{\partial k}{\partial x_i} = P_k - k\omega\check{\beta} + \frac{\partial}{\partial x_i}\left[(\mu + \sigma_k \mu_t)\frac{\partial k}{\partial x_i}\right] \quad (9)$$

Specific dissipation rate:

$$U_i \frac{\partial \omega}{\partial x_i} = \alpha S^2 - \beta\omega^2 + \frac{\partial}{\partial x_i}\left[(\mu + \sigma_{\omega 1}\mu_t)\frac{\partial \omega}{\partial x_i}\right] + 2(1 - F_1)\sigma_{\omega 2}\frac{1}{\omega}\frac{\partial k}{\partial x_i}\frac{\partial \omega}{\partial x_i} \quad (10)$$

Where F_1 is the blending function given by:

$$F_1 = \tanh\left\{\left\{min\left[max\left(\frac{\sqrt{k}}{\check{\beta}\omega y}, \frac{500v}{y^2\omega}\right), \frac{4\rho\sigma_{\omega 2}k}{CD_{k\omega}y^2}\right]\right\}^4\right\} \quad (11)$$

$$CD_{k\omega} = max\left(2\rho\sigma_{\omega 2}\frac{1}{\omega}\frac{\partial k}{\partial x_i}\frac{\partial \omega}{\partial x_i}, 10^{-10}\right) \quad (12)$$

y is the distance to the nearest wall.

The turbulent eddy viscosity for the SST model is defined as follows

$$\mu_t = \frac{a_1 k}{max(a_1\omega, SF_2)} \quad (13)$$

Where S is the vorticity magnitude and the blending function F_2 can be obtained from:

$$F_2 = \tanh\left[\left[max\left(\frac{2\sqrt{k}}{\check{\beta}\omega y}, \frac{500v}{y^2\omega}\right)\right]^2\right] \quad (14)$$

$$y_1 = \frac{\beta_1}{\check{\beta}} - \frac{\sigma_{\omega 1}\lambda^2}{\sqrt{\check{\beta}}}, y_2 = \frac{\beta_2}{\check{\beta}} - \frac{\sigma_{\omega 2}\lambda^2}{\sqrt{\check{\beta}}}. \quad (15)$$

The constants are taken from the ref. [12]:

$\check{\beta} = 0.09, a_1 = 0.31, \lambda = 0.41$

$\beta_1 = 0.075, \sigma_{\omega 1} = 0.5, \sigma_{k1} = 0.85$

$\beta_2 = 0.0828, \sigma_{\omega 2} = 0.856, \sigma_{k2} = 1.0$

3.0 NUMERICAL APPROACH

The computational solution is implemented by employing a commercial pre-processor software – FLUENT 14.0, which is also employed for making the mesh and boundary condition settings while the finite volume method is used to discretize the governing equations. SIMPLE algorithm is used to solve the velocity-pressure coupled equation. The convergence criterion is set to 10^{-6} in order to achieve more accurate convergence.

Penerbit Akademia Baru

Journal of Advanced Research Design
ISSN (online): 2289-7984 | Vol. 4, No.1. Pages 20-27, 2015

4.0 RESULTS AND DISCUSSION

This part introduces a comparison between the simulation results with the three different turbulence models, which are the standard k-ε, the realizable k-ε and the SST k-ω. The goal of this work is not only to validate the CFD model but also to compare the performance of the different turbulence models in terms of mean streamlines and the mean velocity profiles.

4.1 Grid optimization and validation

To confirm the validity and accuracy of the numerical work, three grid densities have been experienced with standard k-ε, which are 150 by 85 and 205 by 105 and 250 by 105. In terms of saving time and accuracy, it was found that the system with grid density of 205 by 105 can be adopted in this computation as shown in Figure (2). In order to prove the validity and precision of the numerical work, the mean velocity profile was compared with the experimental work of Kim [13]. It is shown from Figure (2) that there is a very good agreement between the computed and experimental results, with deviation around 5%.

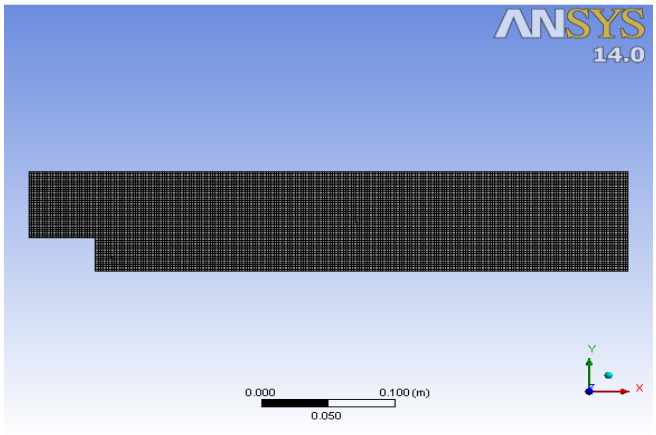

Figure 2: Grid optimization

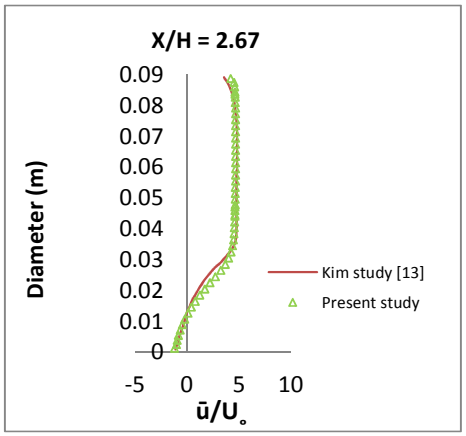

Figure 3: Validation of computed mean velocity profile with experimental work at selected locations

Journal of Advanced Research Design
ISSN (online): 2289-7984 | Vol. 4, No.1. Pages 20-27, 2015

4.2 Comparison of turbulence models

The computed results obtained for the turbulent flow over a backward-facing step for Reynolds number Re = 132,000 and an expansion ratio of 1: 3 were compared with three turbulence models (standard k-ε, realizable k- ε and SST k-ω).

4.2.1 Reattachment length

The computed streamlines obtained from the standard k-ε, realizable k-ε and SST k-ω models are shown in Fig. 4. It can be seen that they all have similar behaviour in terms of separation but there are differences in the reattachment length. SST k-ω clearly indicates a longer reattachment length of L/H = 7.2 compared to the reattachment points of both standard k-ε and realizable k-ε, which are 6 and 6.7, respectively. On the other hand, according to Kim [13], the reattachment point was around L/H=7.1. It is noticed that SST turbulence model results provide good agreement with the experimental work, which might have been due to its high performance in predicting a greater degree of turbulence kinetic energy compared to the other models.

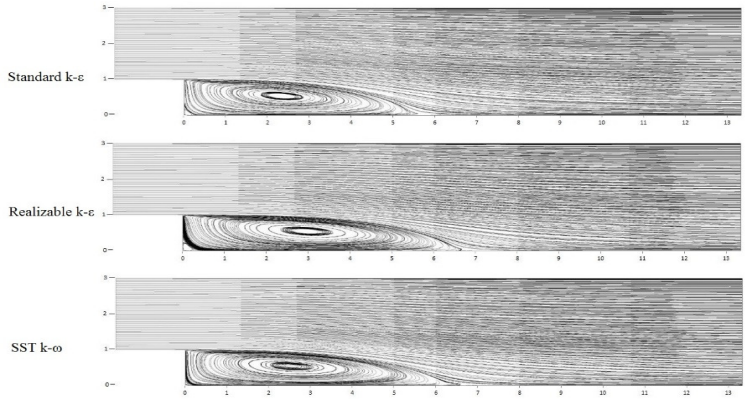

Figure 4: Computed results of streamlines for three turbulent models

4.2.2 Mean velocity profile

All three turbulent models exhibited recirculation regions at different locations behind the step. This attitude can be represented as high velocity gradients as shown in Figure (5a, 5b, 5c, 5d, 5e, 5f) of the mean velocity profile. This behaviour arises from the adverse pressure gradient at the edge of the step due to separation of boundary layers and high turbulent movement. Also it is seen that the velocities are almost zero near to the walls because of the highest shear stress. However, from the results of the velocity profiles in Figure 5, it is shown that the standard k-ε model results are closer to the obtained results of that of the experimental work as compared to the other models at different locations on the x-axis behind the step.

Penerbit Akademia Baru

Journal of Advanced Research Design
ISSN (online): 2289-7984 | Vol. 4, No.1. Pages 20-27, 2015

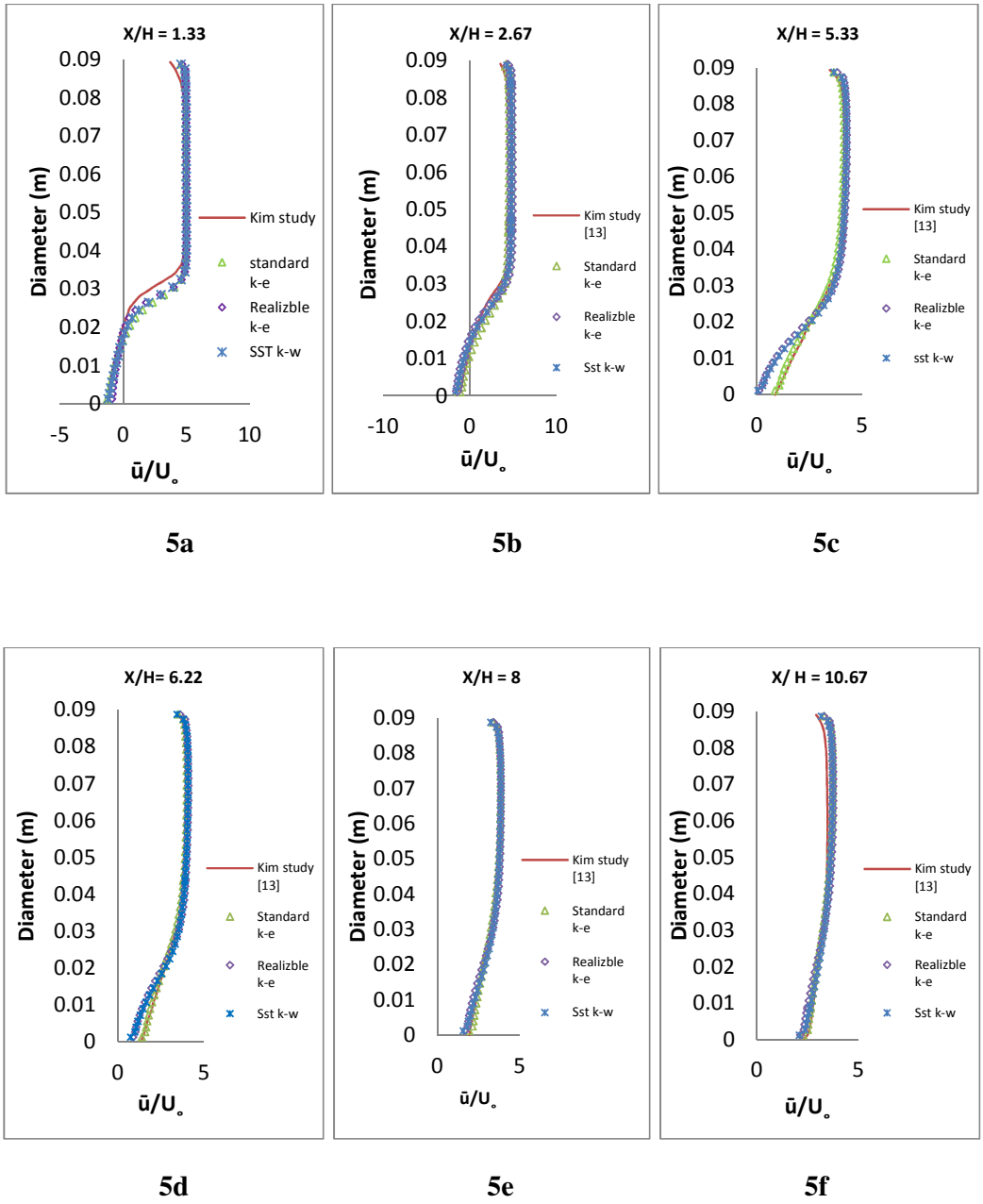

Figure 5: Comparison of the computed mean velocity profiles for three turbulence models with experimental data

4.0 CONCLUSION

In this work, a numerical study of turbulent flows over a backward-facing step has been implemented with three turbulence models (standard k-ε, realizable k-ε and SST k-ω). The SST k-ω model showed very good agreement with experimental data in terms of the length of reattachment regions whereas the standard k-ε model exhibited satisfactory results in terms of mean velocity profile to the experimental data.

REFERENCES

[1] W.C. Lasher, D.B. Taulbee, On the computation of turbulent backstep flow, International Journal of Heat and Fluid Flow 13 (1992) 30-40.

[2] H. Le, P. Moin, J. Kim, Direct numerical simulation of turbulent flow over a backward-facing step, Journal of Fluid Mechanics 330 (1997) 349-374.

[3] B.F. Armaly, F. Durst, J.C.F. Pereira, B. Schönung, Experimental and theoretical investigation of backward-facing step flow, Journal of Fluid Mechanics 127 (1983), 473-496

[4] H. Togun, M.R. Safaei, R. Sadri, S.N. Kazi, A. Badarudin, K. Hooman, E. Sadeghinezhad, Numerical simulation of laminar to turbulent nanofluid flow and heat transfer over a backward-facing step, Applied Mathematics and Computation 239 (2014) 153-170.

[5] M. Shahi, M, J.B. Kok, A. Pozarlik, On characteristics of a non-reacting and a reacting turbulent flow over a backward facing step (BFS), International Communication in Heat and Mass Transfer (2014) 16-25.

[6] J.K. Eaton, J. P. Johnston, (1980). Turbulent flow reattachment: an experimental study of the flow and structure behind a backward-facing step, Stanford University.

[7] S.N. Sinha, A.K. Gupta, M. Oberai, Laminar separating flow over backsteps and cavities. I-Backsteps, AIAA Journal, 19 (1981), 1527-1530.

[8] T. Lee, D. Mateescu, Experimental and numerical investigation of 2D backward-facing step flow, Journal of Fluids and Structures 12(1998) 703-716.

[9] H. Le, P. Moin, J. Kim, Direct numerical simulation of turbulent flow over a backward-facing step, Journal of Fluid Mechanics 330 (1997) 349-374

[10] E.W. Adams, J.P. Johnston, Effects of the separating shear layer on the reattachment flow structure Part 2: Reattachment length and wall shear stress, Experiments in Fluids 6, (1988) 493-499.

[11] B.E. Launder, D.B. Spalding, The numerical computation of turbulent flows, Computer Methods in Applied Mechanics and Engineering 3 (1974), 269-289.

[12] F.R. Menter, Two-equation eddy-viscosity turbulence models for engineering applications, AIAA Journal 32 (1994), 1598-1605

[13] J. Kim, S.J. Kline, J.P. Johnston, Investigation of a reattaching turbulent shear layer: flow over a backward-facing step, Journal of Fluids Engineering 102 (1980) 302-308.

[14] F. Scarano, M. L. Reithmuller, Iterative multigrid approach in pv image processing with discrete window offset, Experiments in Fluids 26 (1999) 513-523.